Supplementary Information

Oxygen-Coordinated MOF Membrane Facilitated Construction of Supported Co_2P/CoP@C Heterostructures for Water Electrolysis

Chongxi Zhang,[a,†] Fengting Li,[a,†] Dong Wu,[a] Qingmeng Guo,[a] Zhanning Liu,[b] Zhikun Wang,[a] Zixi Kang,[a] Lili Fan [a,] and Daofeng Sun [a]*

a School of Materials Science and Engineering, China University of Petroleum (East China), Qingdao 266580, P. R. China.

b School of Materials Science and Engineering, Shandong University of Science and Technology, Qingdao, 266590, P. R. China

† These authors contributed equally to this work.

* Corresponding authors (E-mail: lilifan@upc.edu.cn)

Keywords: water electrolysis; Co_2P/CoP; oxygen-coordinated MOF; electrochemical deposition; HER

1. Experimental details

1.1. Electrochemical measurements

Electrochemical measurements were carried out in a three-electrode system using a Gamry electrochemical workstation. In order to evaluate the catalysts' performance for HER and OER, the prepared samples were used as working electrodes, along with graphite rod as counter electrode and Ag/AgCl (1.0 M KOH) electrode as reference electrode. Polarization curve was obtained with a scan rate of 10 mV s^{-1} and corrected with IR compensation. All the measured potentials versus Ag/AgCl (1.0 M KOH) were converted to reversible hydrogen electrodes (RHE) using the following equation:

$$E_{RHE} = E_{Ag/AgCl} + 0.059pH + E^{\theta}_{Ag/AgCl}$$

Electrochemical impedance spectroscopy (EIS) was performed from 0.01 to 100 kHz. To estimate the electrochemical active surface area (ECSA) of the catalysts, the electrical double-layer capacitor (C_{dl}) was first evaluated by CV in the range of non-Faradaic region at diverse scanning speeds (20 ~ 120 mV s^{-1}). Then, the C_{dl} was obtained based on the following equation:

$$C_{dl} = \frac{Q}{U} = \frac{dQ/dt}{dU/dt} = \frac{j}{r}$$

where Q, U, j, and r stand for the electric charge quantity per unit area, voltage, current density, and scan rate respectively. The ECSA values were calculated according to the following equation:

$$ECSA = \frac{C_{dl}}{C_s}$$

where C_s is a general specific capacitance of 0.04 mF cm^{-2} in 1.0 M alkaline media for metal electrodes.

1.2. DFT calculations

All calculations were performed using the spin-polarized Density Functional Theory (DFT) method implemented in the Vienna Ab initio Simulation Package (VASP). The (100) crystal planes of CoP and Co_2P were selected for investigation. To simulate the interaction between ions and electrons, we employed the Projector Augmented Wave (PAW) technique. For describing the electron exchange-correlation interaction, the Generalized Gradient Approximation (GGA) based on the PBE function was adopted. In the computational setup, the cutoff energy for plane waves was set to 500 eV to ensure the accuracy of the calculations. For structural optimization and electronic structure calculations, k-point grids of 2 × 2 × 1 and 5 × 5 × 1 were used for relaxation and electronic convergence, respectively, to adequately sample the Brillouin zone. To eliminate potential interlayer interactions in the simulation, a vacuum distance of 20 Å was set in the z-direction. Additionally, the empirically corrected DFT-D3 method was employed to account

for van der Waals interactions, providing a more accurate description of intermolecular forces. In terms of convergence criteria, strict standards were set: the force convergence limit per atom was set to 1.0×10^{-5} eV $Å^{-1}$, and the energy convergence limit was set to 0.02 eV. These settings ensured that our simulation results possessed sufficient precision and reliability.

2. Supplemental figures and tables

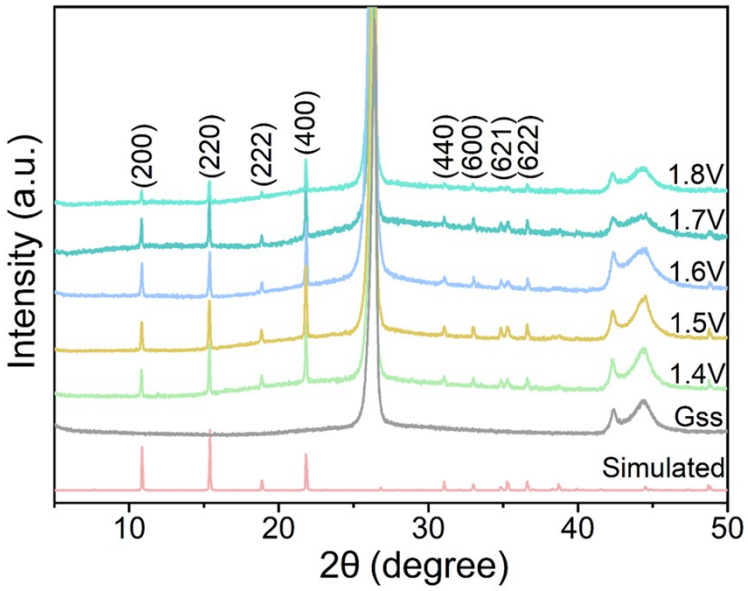

Fig. S1 (a) XRD patterns of Co-squarate MOF membranes prepared at different voltages.

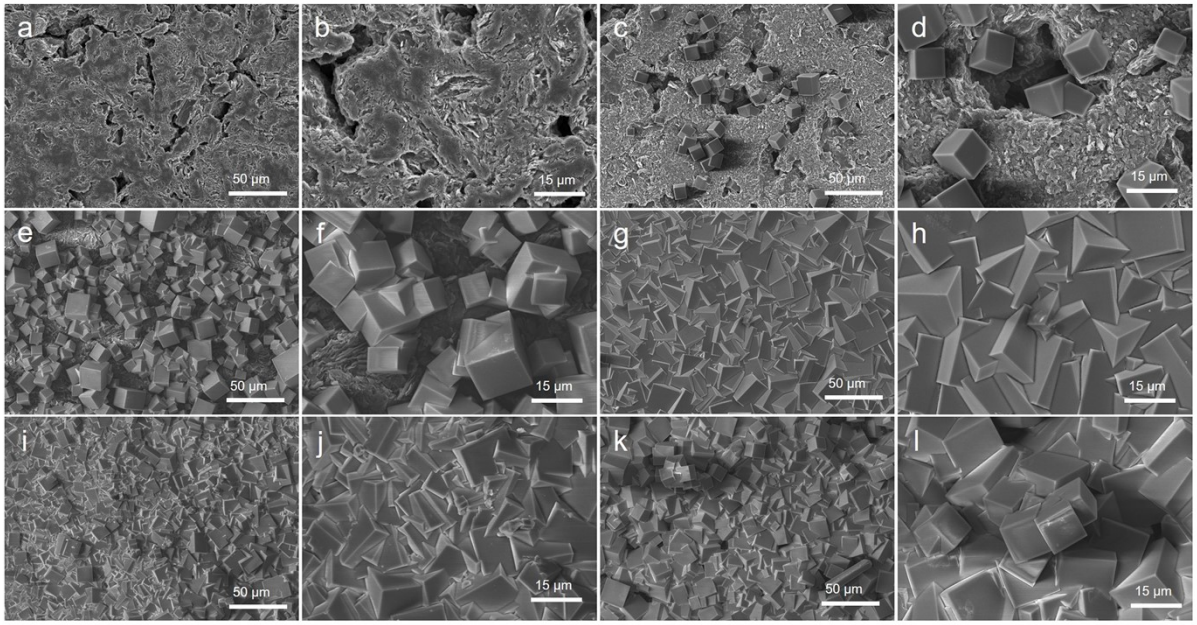

Fig. S2 Top-view SEM images of (a,b) graphite substrate and Co-squarate membrane prepared under different voltages: (c, d) 1.4 V, (e, f) 1.5 V, (g, h) 1.6 V, (i, j) 1.7 V, and (k, l) 1.8V.

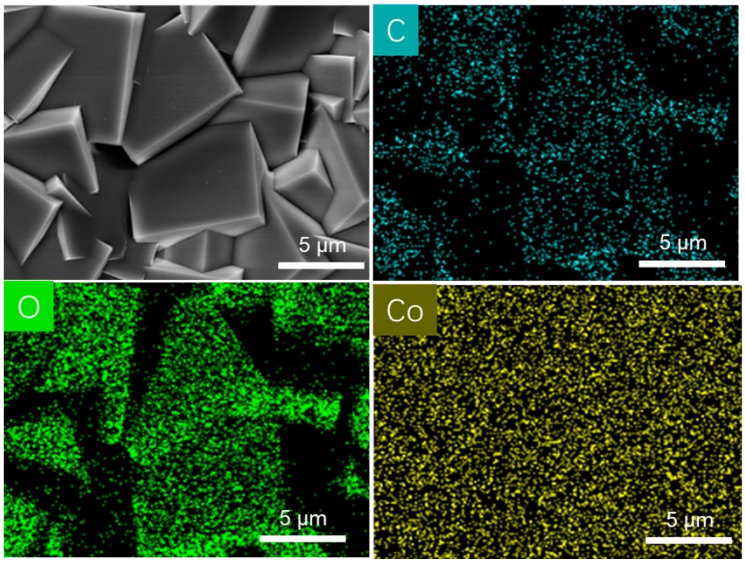

Fig. S3 The elemental mapping images of Co-squarate membrane obtained at 1.6 V.

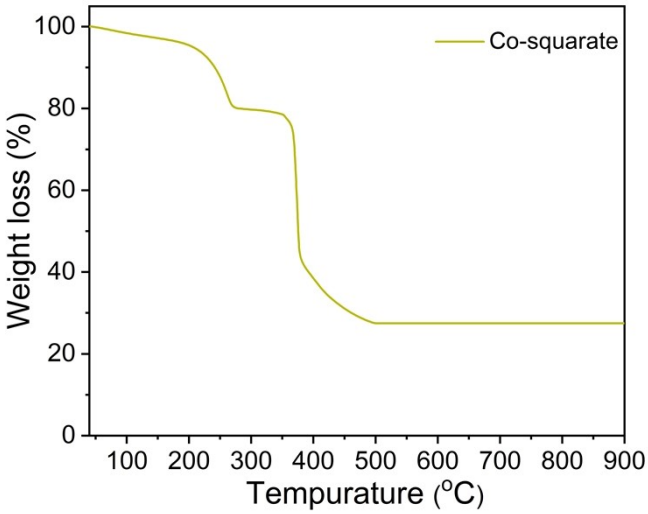

Fig. S4 TGA curve of Co-squarate MOF.

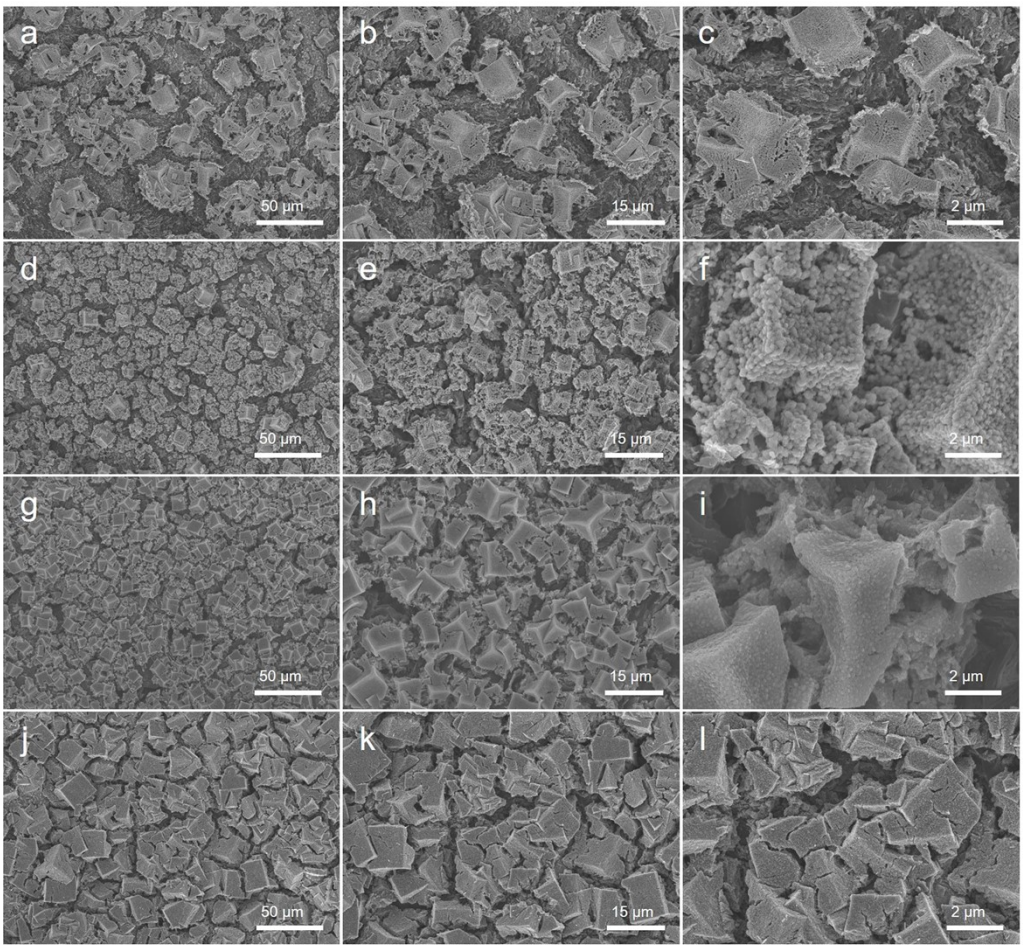

Fig. S5 SEM image of Co-squarate membrane carbonized at different temperatures: (a-c) Gss-Co/CoO@C 600, (d-f) Gss-Co/CoO@C -700, (g-i) Gss-Co/CoO@C-800, and (j-l) Gss-Co/CoO@C-900.

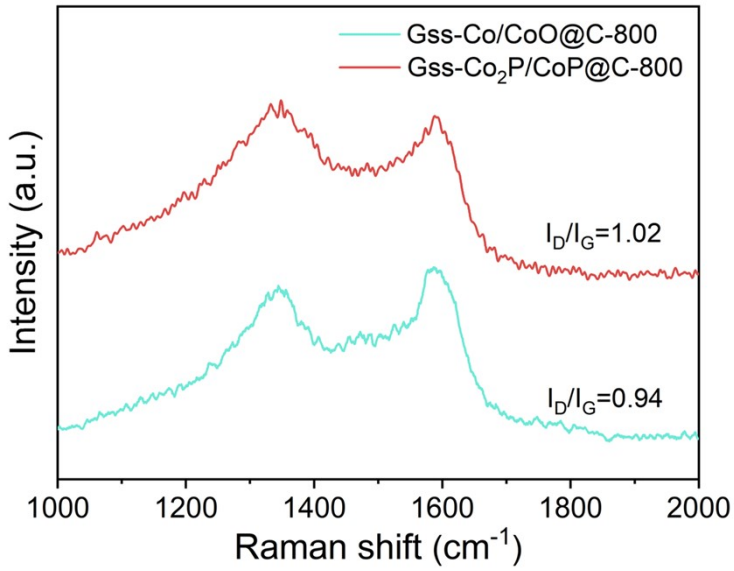

Fig. S6 Raman spectra of Gss-Co/CoO@C-800 and Gss-Co_2P/CoP@C-800.

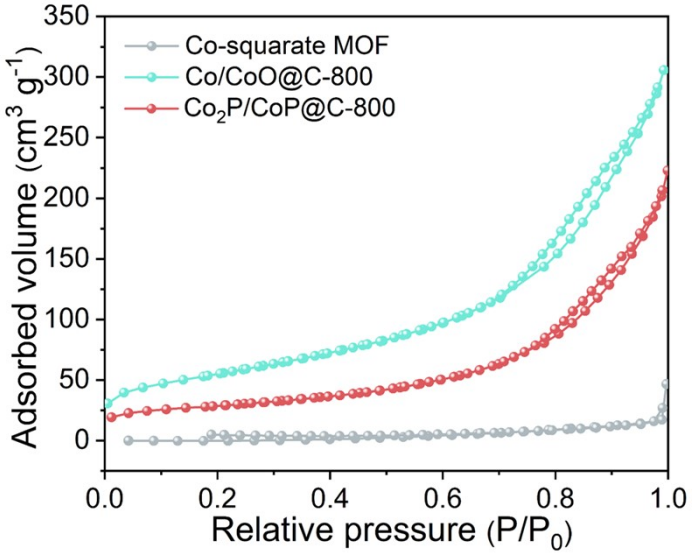

Fig. S7 N_2 adsorption-desorption isotherms of Co-squarate, Co/CoO@C-800 and Co_2P/CoP@C-800 powders.

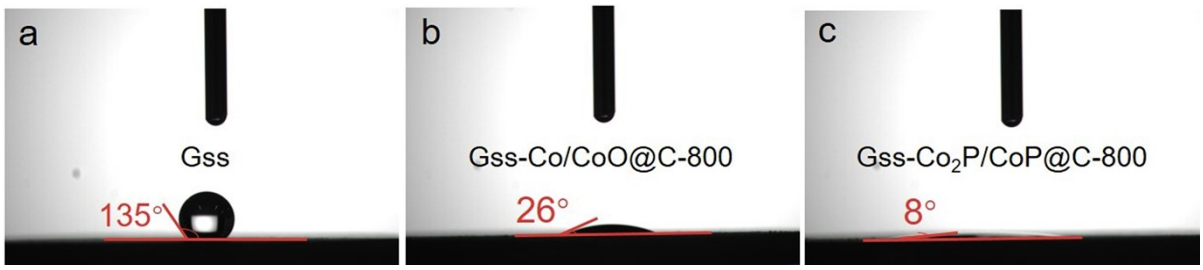

Fig. S8 Water contact-angles of (a) graphite substrate, (b) Gss-Co/CoO@C-800 and (c) Gss-Co_2P/CoP@C-800.

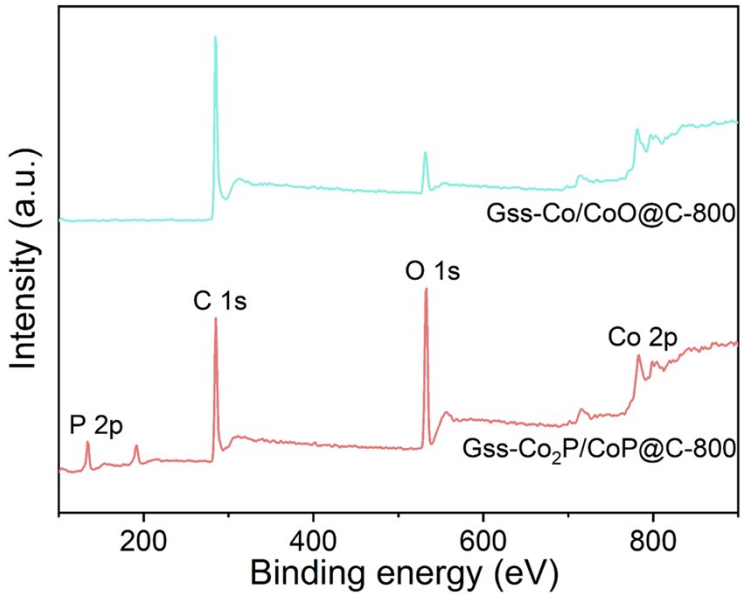

Fig. S9 XPS survey spectra of Co/CoO@C-800 and Co_2P/CoP@C-800 powders.

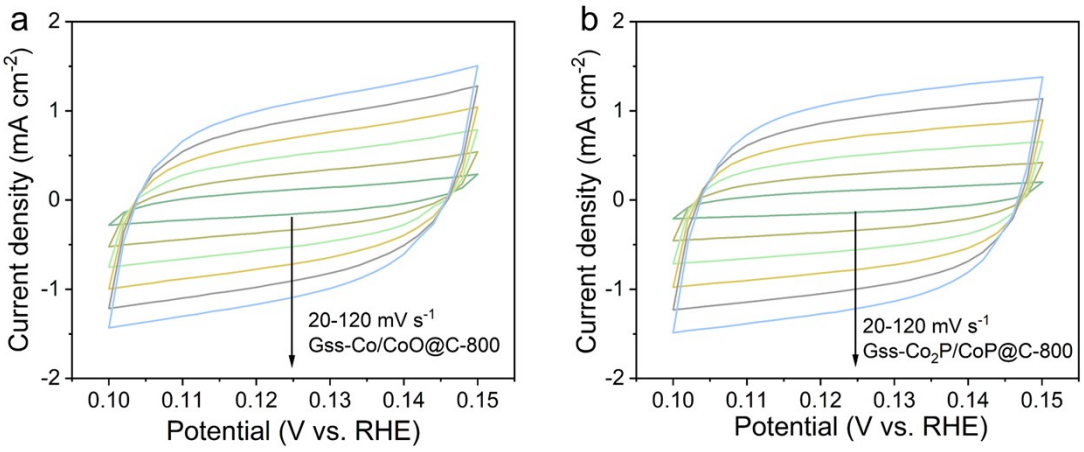

Fig. S10 CVs of the catalysts recorded from 0.10 to 0.15 V at different rates from 20 to 120 mV s^{-1} for (a) Gss-Co/CoO@C-800 and (b) Gss-Co_2P/CoP@C-800 in 1 M KOH for HER.

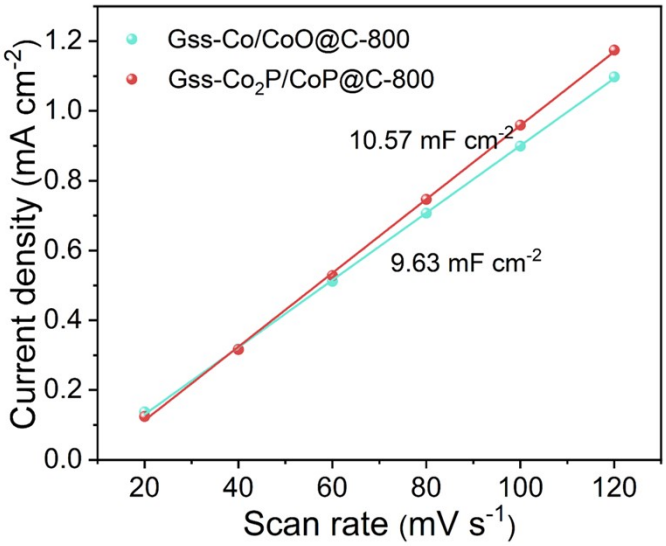

Fig. S11 Double-layer capacitance of Gss-Co/CoO@C-800 and Gss-Co_2P/CoP@C-800 calculated for HER.

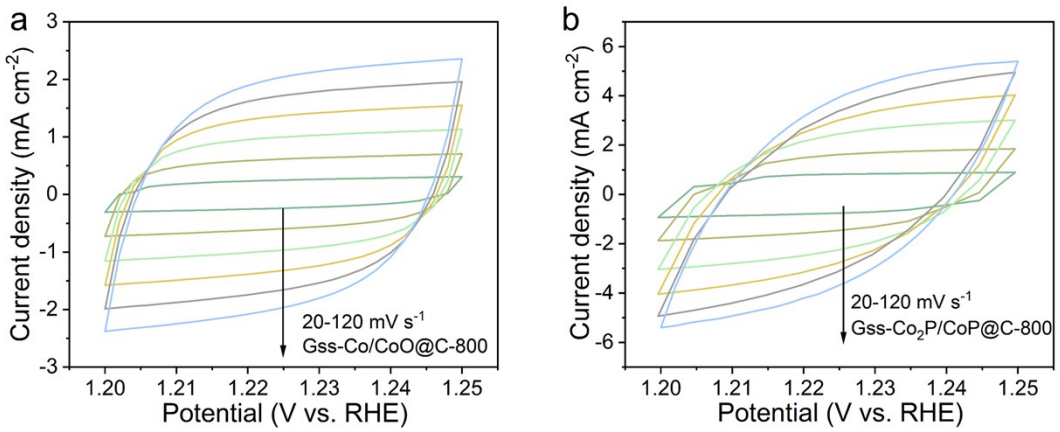

Fig. S12 CVs of the catalysts recorded from 1.2 to 1.25 V at different rates from 20 to 120mV s^{-1} for (a) Gss-Co/CoO@C-800 and (b) Gss-Co_2P/CoP@C-800 in 1 M KOH for OER

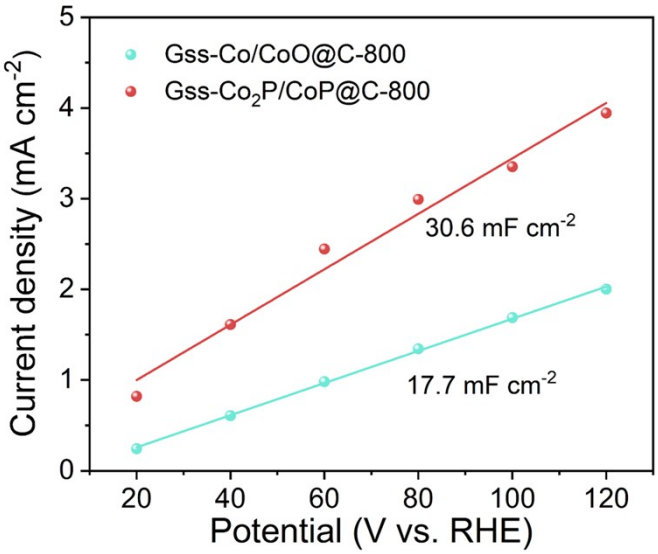

Fig. S13 Double-layer capacitance of of Gss-Co/CoO@C-800 and Gss-Co_2P/CoP@C-800 calculated for OER.

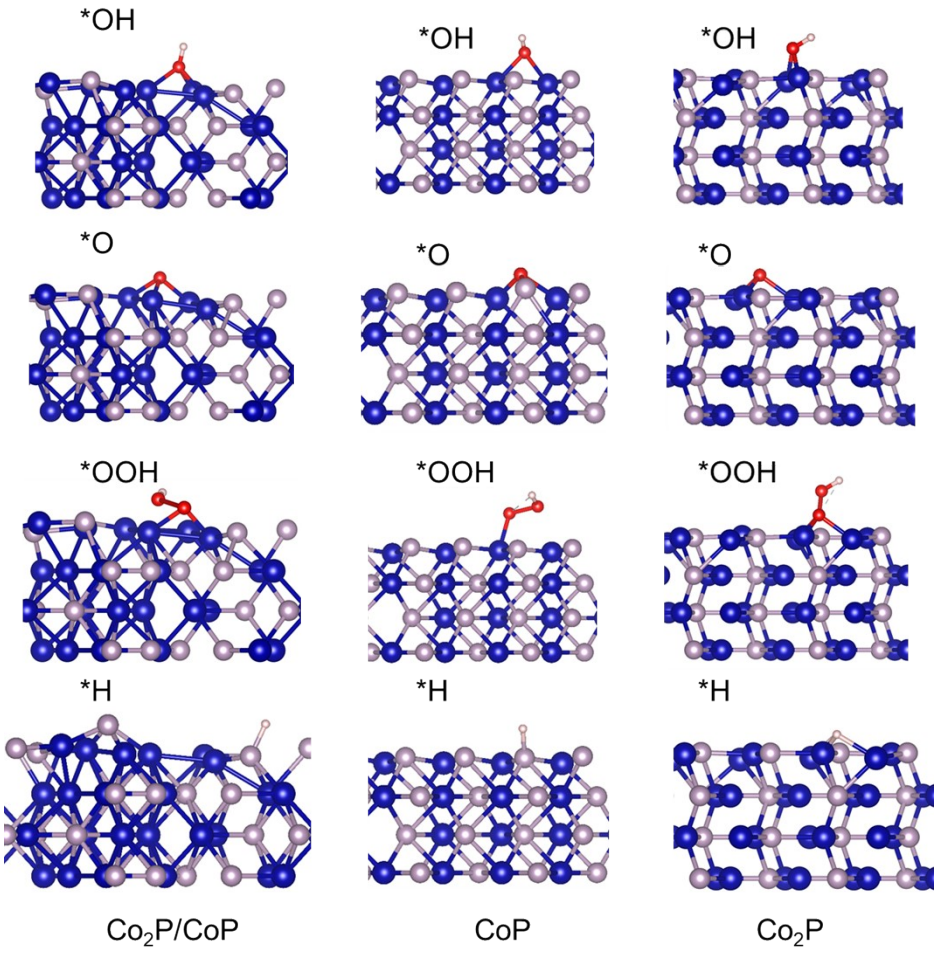

Fig. S14 Optimized adsorption models of Co_2P/CoP, Co_2P and CoP.

Table S1. Co and P contents in different samples measured by ICP-OES.

Catalysts	Co (wt. %)	P (wt. %)
Co-squarate MOF	29.12	-
Gss-Co/CoO@C-800	78.77	-
Gss-Co_2P/CoP@C-800	57.04	16.81

Table S2. Atomic ratios of C, O, Co and P on the surface of as-prepared catalysts.

Catalysts	C (at. %)	O (at. %)	Co (at. %)	P (at. %)
Gss-Co/CoO@C-800	87.12	6.96	3.18	0
Gss-Co_2P/CoP@C-800	58.85	28.7	3.42	9.03

Table S3. The overall water splitting performance of this work compared with recently reported MOF-derived electrocatalysts in alkaline electrolyte.

MOF	MOF-derived electrocatalysts	Cell voltage (V) at 10 mA cm^{-2}	References
Co-squarate	Co_2P/CoP@C	1.54	This work
ZIF-67	Co_2P/CoNPC	1.64	1
ZIF-67@Co-Fe PBA YSMPs	CoP@FeCoP/NC	1.57	2
ZIF-67	CoP@NC	1.69	3
Co-MOFs@XC-72	CoPS@NPS-C	1.62	4
Zn-Co@MOF-CNT/CC	ZnP_2@CoP-CNT/CC	1.53	5
Co-MOF/NF	CoP/NF	1.54	6
Co-MOF/CC	NiFeCoP/CC	1.62	7
MOF(nf)	NiCo(nf)-P	1.74	8
ZIF-67	NC/Co/CoP/CP	1.72	9
Co-MOF	CoP-NC@NFP	1.64	10
Cu-NiCo-MOF	M -NiCoP	1.68	11

CoFc-MOF	Co_2P-FeP@C-5	1.66	12
CoFe PBA NFs	Fe-CoP NFs	1.65	13
Co ZIF-L	CoP@NPCNTs/CTs	1.50	14
Co-ZIF-L@PDA	Co_2P-NC	1.648	15
ZIF-67@ MIL-101/CP	CoP/FeP/CP	1.62	16

REFERENCES

1. H. Liu, J. Guan, S. Yang, Y. Yu, R. Shao, Z. Zhang, M. Dou, F. Wang and Q. Xu, Metal-organic-framework-derived Co_2P nanoparticle/multi-doped porous carbon as a trifunctional electrocatalyst, *Adv. Mater.*, 2020, **32**, 2003649.
2. J. Shi, F. Qiu, W. Yuan, M. Guo and Z.-H. Lu, Nitrogen-doped carbon-decorated yolk-shell CoP@FeCoP micro-polyhedra derived from MOF for efficient overall water splitting, *Chem. Eng. J.*, 2021, **403**, 126312.
3. Z. Li, J. Sui, Q. Zhang, J. Yu, L. Yu and L. Dong, CoP@NC electrocatalyst promotes hydrogen and oxygen productions for overall water splitting in alkaline media, *Int. J. Hydrogen Energy*, 2021, **46**, 2095-2102.
4. Y. Hu, F. Li, Y. Long, H. Yang, L. Gao, X. Long, H. Hu, N. Xu, J. Jin and J. Ma, Ultrafine CoPS nanoparticles encapsulated in N, P, and S tri-doped porous carbon as an efficient bifunctional water splitting electrocatalyst in both acid and alkaline solutions, *J. Mater. Chem. A*, 2018, **6**, 10433-10440.
5. M. Afshan, P.K. Sachdeva, D. Rani, S. Das, M. Pahuja, S.A. Siddiqui, S. Rani, R. Ghosh, N. Chaudhary, Jyoti, S. Riyajuddin, C. Bera and K. Ghosh, Porous Carbon Template Decorated with MOF-Driven Bimetallic Phosphide: A Suitable Heterostructure for the Production of Uninterrupted Green Hydrogen via Renewable Energy Storage Device, *Small*, 2023, **19**, 2304399.
6. J. Liu, Y. Gao, X. Tang, K. Zhan, B. Zhao, B.Y. Xia and Y. Yan, Metal–organic framework-derived hierarchical ultrathin CoP nanosheets for overall water splitting, *J. Mater. Chem. A*, 2020, **8**, 19254-19261.
7. M. Xiao, L. Jiao, D. Xiang, P. Gao, J. Fu, A. Naseri and S. Huang, Synergistic electronic structure tuning of self-assembled hollow hierarchical Ni-Fe-Co-P nanowire arrays on carbon cloth for enhanced water splitting, *J. Alloys Compd.*, 2023, **968**, 171883.
8. Z. Xu, C.-L. Yeh, J.-L. Chen, J.T. Lin, K.-C. Ho and R.Y.-Y. Lin, Metal–Organic Framework-Derived 2D NiCoP Nanoflakes from Layered Double Hydroxide Nanosheets for Efficient Electrocatalytic Water Splitting at High Current Densities, *ACS Sustainable Chem. Eng.,* 2022, **10**, 11577-11586.

9. M. Cong, D. Sun, L. Zhang and X. Ding, In situ assembly of metal-organic framework-derived N-doped carbon/Co/CoP catalysts on carbon paper for water splitting in alkaline electrolytes, *Chin. J. Catal.*, 2020, **41**, 242-248.
10. E. Vijayakumar, S. Ramakrishnan, C. Sathiskumar, D.J. Yoo, J. Balamurugan, H.S. Noh, D. Kwon, Y.H. Kim and H. Lee, MOF-derived CoP-nitrogen-doped carbon@NiFeP nanoflakes as an efficient and durable electrocatalyst with multiple catalytically active sites for OER, HER, ORR and rechargeable zinc-air batteries, *Chem. Eng. J.*, 2022, **428**, 131115.
11. Q. Wang, C. Wang, X. Du and X. Zhang, Controlled synthesis of M (M = Cr, Cu, Zn and Fe)-NiCoP hybrid materials as environmentally friendly catalyst for seawater splitting, *J. Alloys Compd.,* 2023, **966**, 171516.
12. Z. Li, Z. Li, H. Yao, Y. Wei and J. Hu, Bifunctional Co_xP-FeP@C for overall water splitting realized by manipulating the electronic states of Co via phosphorization, *J. Colloid Interface Sci.*, 2024, **653**, 857-866.
13. Y. Yuan, K. Wang, B. Zhong, D. Yu, F. Ye, J. Liu, J. Dutta and P. Zhang, MOF-Derived Iron-Cobalt Phosphide Nanoframe as Bifunctional Electrocatalysts for Overall Water Splitting, *Energy Environ. Mater.*, 2024, **7**, e12747.
14. D. Kong, Q. Xu, N. Chu, H. Wang, Y.V. Lim, J. Cheng, S. Huang, T. Xu, X. Li, Y. Wang, Y. Luo and H.Y. Yang, Rational Construction of 3D Self-Supported MOF-Derived Cobalt Phosphide-Based Hollow Nanowall Arrays for Efficient Overall Water Splitting At large Current Density, *Small*, 2024, **20**, 2310012.
15. H. Xue, Z. Zhang, Y. Lai, H. Gong, S. Zhang, W. Xia, J. Li and J. He, Construction of Co_2P nanoparticles anchored on hollow N-doped porous carbon nanoleaf for high-efficiency water splitting. *Chem. Eng. J.*, 2024, **483**, 149057.
16. L. Zeng, L. An, Z. Zhang, J. Zheng, W. Chen, C. Liu, Y. Zheng, D. Dang and Z.-Q. Liu, Heterogeneous strategy constructing a built-in electric field: CoP/FeP bifunctional electrode for overall water splitting. *Chem. Eng. J.*, 2024, **491**, 152084.